Resonant sum-difference frequency mixing enhanced by electromagnetically induced transparency in krypton

C. Dorman* and J. P. Marangos
Laser Optics and Spectroscopy Group, Blackett Laboratory, Imperial College of Science, Technology and Medicine, London SW7 2BZ, United Kingdom
(Received 2 March 1998)

We report experiments that investigate the generation of coherent VUV radiation at 123.6 nm via a resonant sum-difference frequency mixing scheme in Kr. One of the mixing fields at 212.55 nm was in two-photon resonance with the transition between the $4p^6\ ^1S$ ground state and the $4p^5\ 5p[0,\frac{1}{2}]$ excited state (94 093.7 cm^{-1}). The second field (the coupling field) at 759 nm was in single-photon resonance with the transition between the $4p^5\ 5p[0,\frac{1}{2}]$ state and the $4p^5\ 5s[1,\frac{1}{2}]$ state at 80 917.6 cm^{-1}. The presence of the coupling field leads to electromagnetically induced transparency (EIT) at the wavelength of the generated field, 123.6 nm. This is predicted to enhance the four-wave-mixing efficiency by a large factor. We have studied the dependence of the four-wave mixing process on the detuning and strength of the coupling field. The efficiency for four-wave mixing was found to be enhanced by a significant factor (>5) by the EIT effect when the resonant coupling field strength exceeded about half the Doppler width (0.1 cm^{-1}). A calculation for monochromatic fields and a uniform slab of gas provided qualitative agreement with the results of experiment. The relative conversion efficiency for this resonant mixing scheme is found to be 10^4 times greater than that for a similar scheme where the coupling laser is tuned far (1270 cm^{-1}) off resonance. A substantial part of this resonant enhancement can thus be attributed to the EIT effect. [S1050-2947(98)00511-3]

PACS number(s): 42.65.Ky, 42.50.Gy, 42.50.Hz

I. INTRODUCTION

Nonlinear optical processes are used to generate coherent radiation at frequencies beyond those where lasers normally operate. For example, frequency doubling in optical crystals of tunable (pulsed or cw) laser light in the visible range can be used to provide bright sources of tunable coherent radiation in the ultraviolet (UV) range of the spectrum (400–200 nm). Likewise, in the infrared range (1.0–5.0 μm) optical-parametric conversion in optical crystals is widely used to down-convert coherent light from the visible/near IR region. Frequency mixing in optical crystals can be very efficient, with the energy conversion efficiency from fundamental to the new wavelength being $\sim$0.1–0.5 or more. High conversion efficiencies are obtained since in the operating range of these crystals they have a high nonlinear susceptibility while remaining transparent, and good phase matching can be maintained over lengths of many tens of millimeters by using the birefringent properties of these crystals [1].

In the vacuum ultraviolet (VUV) ($<$190 nm) no transparent nonlinear optical crystals exist and to generate coherent radiation via nonlinear up-conversion in this wavelength range requires the use of atomic and molecular gases and vapors. Four-wave mixing of pulsed laser radiation in atomic gases has been developed over the past two decades [2], with various techniques being employed, for example nonresonant third-harmonic generation (THG) [3], parametric stimulated Raman up-conversion [4], and two-photon resonance enhanced sum and sum-difference frequency mixing [5,6]. The last of these methods has been particularly successful because it provides, from a single atomic mixing scheme, a wide spectral coverage with a two-photon resonantly enhanced nonlinear susceptibility. Conversion efficiencies of up to $\sim 10^{-4}$ are routinely possible with these methods, and by introduction of buffer gases to optimize phase matching further increases of conversion efficiency to $>10^{-4}$ ([6], for example, corresponding to peak powers of $>$100 W at 121.6 nm) can be achieved.

Despite these demonstrations the conversion efficiencies obtained via four-wave mixing in atomic and molecular gases remain very small compared to the conversion efficiencies achieved in nonlinear optical crystals. The reasons for this are that the per atom nonlinear susceptibility is generally low in these schemes since the generated field is usually detuned from any allowed atomic transition. This requirement for the generated field wavelength along with the much lower atom densities in a gas compared to a solid-state medium, results in the small conversion efficiencies. Resonant enhancement can be used to improve the conversion efficiency through an increase in the nonlinear susceptibility. If the generated field is near resonance, however, the increased nonlinear susceptibility will be associated with undesirable high absorption and high dispersion. Thus both the absorption length (over which the generated field is absorbed) and coherence length (over which phase matching is maintained) will be very short in this case. At typical atom densities of 10^{16} cm^{-3} these lengths will be on the order of ~ 1 μm, leading to a reduced advantage in resonant frequency mixing despite the large nonlinear susceptibility. So although there can be an increase in conversion efficiency by working at resonance the full potential of this will not, in general, be exploitable.

A way to enhance greatly the conversion efficiencies in

*Electronic address: c.dorman@ic.ac.uk

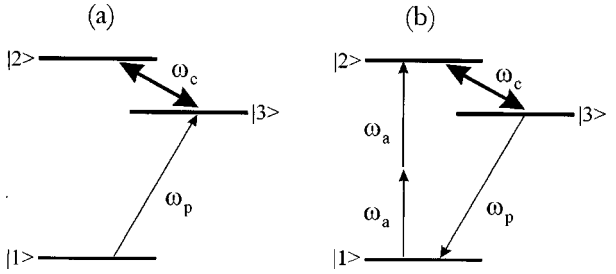

FIG. 1. (a) shows the standard configuration for a ladder EIT scheme in a three-level atomic system. The ground state $|1\rangle$ is dipole coupled to $|3\rangle$ but not to $|2\rangle$; $|2\rangle$ is dipole coupled to $|3\rangle$. If a coupling field of frequency ω_C is applied to the $|2\rangle$-$|3\rangle$ transition a probe field at frequency ω_P applied resonantly to the $|1\rangle$-$|3\rangle$ transition will experience reduced absorption due to EIT. (b) shows how the same energy level scheme can be incorporated into a resonant four-wave mixing scheme that generates a field at ω_P. In this mixing scheme an additional field at ω_a, in two-photon resonance with the $|1\rangle$-$|2\rangle$ interval, is applied along with the single-photon resonant coupling field ω_C, which induces transparency for the radiation generated at $2\omega_a-\omega_C=\omega_{31}$.

resonant four-wave mixing schemes was proposed by Harris, Field, and Imamoglu in 1990 [7]. The key to this proposal was to create a laser dressed medium for which the nonlinear susceptibility remains resonantly enhanced while the linear susceptibility is reduced to very small values. This scheme utilizes laser-induced quantum interference or electromagnetically induced transparency (EIT) to cause the destructive interference of the amplitudes associated with the resonant linear susceptibility while the amplitudes associated with nonlinear susceptibility see constructive interference.

EIT processes can occur in a three-level atomic system in the ladder or Λ configurations, i.e., comprising a ground state $|1\rangle$, an excited state $|3\rangle$ dipole coupled to $|1\rangle$, and an excited state $|2\rangle$ that is dipole coupled to $|3\rangle$ but not to $|1\rangle$ [Fig. 1(a)]. We consider the situation when two laser fields, frequencies ω_P and ω_C, are applied to this system close to resonance, where ω_P is a weak probe field (strength Ω_P) on the $|1\rangle$-$|3\rangle$ transition and ω_C is a strong coupling field (strength Ω_C) on the $|2\rangle$-$|3\rangle$ transition. Assuming that there is negligible population in the upper states $|2\rangle$ and $|3\rangle$ throughout the process, any changes in absorption will be due to the effects of interference and not population changes. In the limit of $\Omega_C \gg \gamma > \Omega_P$ (where γ is the larger radiative decay rate in the three-level system, i.e., spontaneous decay of state $|3\rangle$) the interaction between the coupling field and the atom must be viewed as inherently nonperturbative. A useful basis within which to view this situation is the dressed-state basis [8]. The dressed states formed when the coupling field is resonant $(\omega_{23}-\omega_C=0)$ are coherent superpositions of the two upper states $|2\rangle$ and $|3\rangle$:

$$|a\rangle=(1/\sqrt{2})[|2\rangle+|3\rangle], \tag{1a}$$

$$|b\rangle=(1/\sqrt{2})[|2\rangle-|3\rangle]. \tag{1b}$$

The amplitude for a transition at the (undressed) resonant frequency $(E_3-E_1)/\hbar$ from the ground state $|1\rangle$ to the dressed states will be the sum of the contributions to states $|a\rangle$ and $|b\rangle$. Assuming $|2\rangle$ to be metastable, the contributions from the $|1\rangle$-$|3\rangle$ transition cancel since they enter the sum with opposite signs. The cancellation of absorption on the $|1\rangle$-$|3\rangle$ transition can equivalently be viewed in terms of Fano type interference [9,10].

The basic EIT ladder scheme of Fig. 1(a) can be incorporated within a resonant four-wave mixing scheme [Fig. 1(b)] if an additional field, frequency ω_a, is applied in two photon resonance with the $|1\rangle$-$|2\rangle$ transition (i.e., $\omega_{12}=2\omega_a$). In this case the field generated in the four-wave mixing process will be at frequency $\omega_g=\omega_{31}$. Therefore this frequency mixing scheme not only uses two-photon resonance on the $|1\rangle$-$|2\rangle$ transition (as already much investigated [5,6]), but also single-photon resonance on the $|2\rangle$-$|3\rangle$ transition. In the laser dressed medium the susceptibilities will be of the form shown in Fig. 2 (these are discussed in detail in Sec. II). If the coupling laser strength Ω_C is a few times larger than the Doppler width in the medium then Re $\chi_D^{(1)}$ and Im $\chi_D^{(1)}$ at resonance will be reduced to very small values. Thus the absorption and coherence lengths will become much larger at resonance than in the undressed case. The increase in the absorption length will be from values of a few micrometers to many millimeters in a medium of number density 10^{16}–10^{17} cm^{-3}. $\chi_D^{(3)}$ will, in contrast to the linear terms, be subject to constructive interference and so will still display a degree of resonant enhancement giving a high value for the per atom susceptibility. The combined effect of the increased nonlinear susceptibility and the greatly increased absorption and coherence lengths leads to an enhanced conversion efficiency for the four-wave mixing scheme. The generated field is produced with an intensity determined, in the limit of a long medium, by a factor proportional to $|\chi_D^{(3)}/\chi_D^{(1)}|^2$. Calculations made for plausible experimental conditions predict this factor to be increased by 10^4 between the undressed and dressed limits [7].

These quantum interference induced enhancements in frequency mixing conversion efficiencies can be realized in a practical scheme, providing that the phases of the coherences induced by the coupling laser can be sufficiently preserved during the interaction time. For a pulsed laser experiment this amounts to the requirement that the laser field be single-mode and transform limited. It is also required that the collisional dephasing and other dampings of the state $|2\rangle$ lifetime (e.g., photoionization) are maintained at levels such that they do not exceed the leading spontaneous decay rates in the system.

Experimental demonstrations of EIT effects on the linear susceptibility (absorption) in strontium and also lead were provided in 1991 [11,12]. These experiments confirmed the effectiveness of laser-induced quantum interference by increasing the transmission of an initially opaque medium by factors of more than e^{10}. The EIT effect on phase matching (i.e., to cause good phase matching) was demonstrated in Stanford in a lead four-wave mixing scheme [13]. This was shown to enhance the conversion efficiency of the generated 283-nm ultraviolet radiation by a factor of 50 compared to the weak field limit. Theoretical work by Harris and Luo [14] has established a condition for the preparation energy (equivalent preparation time) required to create transparency. To create EIT the laser pulse energy must exceed $\hbar\omega$ times the product of the atom number and the ratio of probe to coupling oscillator strengths.

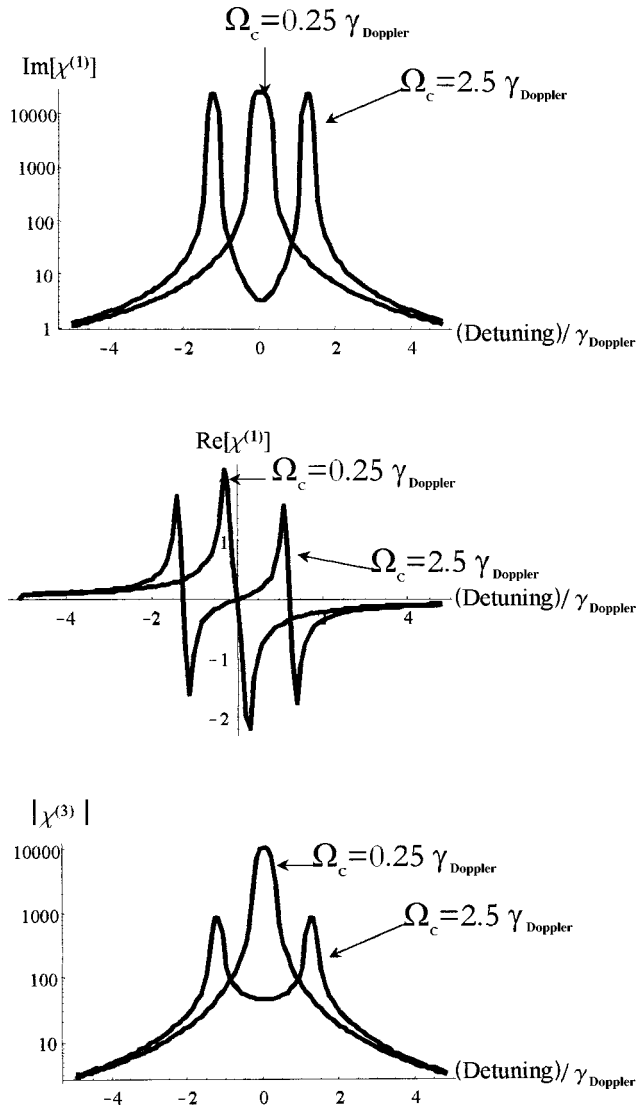

FIG. 2. The calculated Doppler averaged dressed susceptibilities $\mathrm{Im}[\chi_D^{(1)}]$ (top), $\mathrm{Re}[\chi_D^{(1)}]$ (middle), and $|\chi_D^{(3)}|$ (lower) are shown as a function of detuning Δ_g (normalized to the Doppler width) for the Kr four-wave-mixing scheme. The coupling laser is in single-photon resonance $\Delta_C=0$ in these plots. The results shown are for the cases of a coupling Rabi frequency set at $\Omega_C=0.25\gamma_{\mathrm{Doppler}}$ and $\Omega_C=2.5\gamma_{\mathrm{Doppler}}$. In the plots of $\mathrm{Im}[\chi_D^{(1)}]$ and $|\chi_D^{(3)}|$ a logarithmic vertical scale in arbitrary units has been used. For $\mathrm{Re}[\chi_D^{(1)}]$ a linear scale is used.

EIT enhanced nonlinear frequency mixing was first demonstrated in hydrogen by Zhang and co-workers [15]. In this and subsequent experiments [16,17] a microwave discharge source was used to provide a beam of H atoms with high values of the density-length product. This parameter was as high as 3×10^{15} cm^{-2} in these experiments. A laser at 243 nm excited the $1s$-$2s$ two-photon transition while a strong, single-mode, coupling field at 656 nm was applied at resonance to the $2s$-$3p$ transition. Both laser fields were obtained from single-mode pulsed dye lasers. In this scheme resonant enhanced four-wave mixing occurred in the presence of EIT, with a generated field at 103 nm near the $3p$-$1s$ transition. The generated field intensity was produced with a conversion efficiency of 2×10^{-4}. Further increase in conversion efficiency may be possible but would require increased density-length products, something difficult to achieve in a hydrogen beam. More recently [18] these authors have reported EIT enhanced XUV radiation produced in the wavelength region 97.3–92.6 nm by utilizing the $2s$-np resonances in H ($n=4-8$).

We have investigated a resonant frequency mixing scheme in Kr that generates VUV radiation at the wavelength of 123.6 nm. The energy levels of Kr form a three-level system between the ground state $4p^6\ {}^1\mathrm{S}|1\rangle$ at 0 cm^{-1}, the excited state $4p^5\ 5p[0,\frac{1}{2}]|2\rangle$ at 94 093.7 cm^{-1} (which is not accessible by a single photon transition from $|1\rangle$) and the state $4p^5\ 5s[1,\frac{1}{2}]|3\rangle$ at 80 917.6 cm^{-1}, which is dipole coupled to both $|1\rangle$ and $|2\rangle$. In the sum-difference mixing scheme involving these three levels, the two-photon resonant field must be tuned to 212.55 nm and the coupling field to 758 nm. In contrast to the sum mixing experiments in H this is a sum-difference scheme, although this should make no difference, in principle, to the EIT effects that occur. More significantly, however, krypton is available as a monatomic gas that can provide arbitrarily large density-length products. Thus optimal values of density and length can, in principle, be used. The experiments reported here were all performed in a Kr gas jet provided by a pulsed gas valve.

We have studied in particular the dependence of the generated VUV intensity as a function of the two-photon resonant and coupling laser field strengths. The dependence of the latter has been studied over a range of the density-length (NL) product and for various detuning values for the coupling laser. These results show the effects of the laser dressing on four-wave mixing. An appreciable enhancement in the conversion efficiency was apparent at values of the coupling field strength $\gtrsim0.03$ cm^{-1}. This corresponds to the estimated preparation energy condition [14] but is less than the 0.1 cm^{-1} Doppler width. The enhancement due to EIT on the frequency mixing efficiency was found to be by a factor of 5 or more. Further, a measurement was made of the relative enhancement in the conversion efficiency on resonance compared to a measurement made under otherwise identical conditions but with the coupling laser tuned far off resonance (1270 cm^{-1}) (but two-photon resonance maintained). The resonant case showed a factor of 10^4 higher conversion efficiency than the off-resonant case. Thus we can conclude that the EIT effect plays a significant role in the resonant enhancements established in this experiment.

The remainder of this paper takes the following form. In Sec. II we briefly review the method used to calculate the laser dressed susceptibilities and to compute their Doppler averaged values and to calculate the intensity of generated light. In Sec. III our experimental apparatus and method is described. Section IV then presents the results of these measurements and these are then discussed in Sec. V.

II. CALCULATION OF DRESSED SUSCEPTIBILITIES AND FOUR-WAVE MIXING

We will discuss now the calculation of susceptibilities in a three-level atom with levels $|1\rangle$, $|2\rangle$, and $|3\rangle$ forming a ladder system, coupled by fields as shown in Fig. 1(b) so as to result in four-wave mixing. The susceptibilities were found by solving the equations of motion of the density matrices of the atom under steady-state conditions. After Doppler aver-

aging the resulting susceptibilities were used in a propagation calculation to yield the dependence of the generated VUV signal on various parameters that can be compared with the experiment results. A fuller description of the method used can be found in [19], and here we will provide only an outline.

The Hamiltonian of the system is of the form

$$H = H_0 + V, \tag{2}$$

where H_0 is the unperturbed atomic Hamiltonian

$$H_0 = \hbar\omega_1|1\rangle\langle 1| + \hbar\omega_2|2\rangle\langle 2| + \hbar\omega_3|3\rangle\langle 3| \tag{3}$$

and the Hamiltonian for the interaction with the electromagnetic fields is V:

$$V = \hbar\Omega_a \exp(-i2\omega_a t)|2\rangle\langle 1| + \hbar\Omega_C \exp(-i\omega_C t)|2\rangle\langle 3| + \hbar\Omega_g \exp(-i\omega_g t)|3\rangle\langle 1|. \tag{4}$$

Ω_a is the effective two-photon Rabi frequency arising from the two-photon resonant field at frequency ω_a, Ω_C is the coupling field Rabi frequency, and Ω_g is the Rabi frequency of the generated field [where $\hbar\Omega_i = \mu_i|E(\omega_i)|$].

The evolution of each density matrix element is described by the Liouville equation

$$\hbar\frac{\partial\rho_{nm}(t)}{\partial t} = -i\sum_{\mathrm{k}} H_{nk}(t)\rho_{km}(t) + i\sum_{\mathrm{k}} \rho_{nk}(t)H_{km}(t) + \Lambda_{nm}, \tag{5}$$

where Λ_{nm} in Eq. (5) is a phenomenological decay term. This system of equations can be solved to yield values for each of the matrix elements. To do this the rotating-wave approximation is made and the terms in the equations of motion are transformed into a rotating frame such that all of the frequencies are eliminated with the exception of the detunings:

$$\Delta_a = \omega_{13} - 2\omega_a, \quad \Delta_C = \omega_{32} - \omega_C, \quad \Delta_g = \omega_{21} - \omega_g. \tag{6}$$

These detunings are one of the key parameters that can be varied during an experiment.

Further it is assumed that the system is closed so that the population sum $\rho_{11}+\rho_{22}+\rho_{33}=1$. In the conditions of the experiment $\Omega_C \gg \Omega_a, \Omega_g$ and also, in practice, it is always true that $\rho_{11} \gg \rho_{22}, \rho_{33}$. In the calculations considered here the matrix elements are calculated in the steady-state limit. All fields, other than Ω_C, are assumed to be weak so their effects are usually only retained up to first order. But Ω_C is retained to all orders in the calculation. An exception to this was in the calculation of the dependence of the four-wave mixing on the field strength Ω_a, for these higher-order terms were also retained for this parameter. A set of differential equations of the form (5) [19] is obtained. These can be solved in the steady-state limit by a straightforward inversion of what reduces to an 8×8 matrix. This inversion was performed using MATHEMATICA.

The phenomenological dampings in Eq. (5) include the spontaneous decay rates appropriate for these states of Kr. The effects of collisions and photoionization on these damping rates were, however, ignored. The omission of collisional dampings is consistent with their expected values in this system under the density conditions likely ($<10^{17}$ cm^{-3}), being at least an order of magnitude less [20] than the leading spontaneous decay rates. Photoionization of state $|2\rangle$ will occur under the experimental conditions due to the presence of the field at ω_a but is found to be still significantly smaller than spontaneous decay rates of $|3\rangle$ (see Sec. IV). Monochromatic fields are assumed in this calculation of the density matrix. Inserting a laser linewidth into a steady-state calculation, for instance, by adding an additional phenomenological decay due to Wiener-Levy phase diffusion [21] of the fields, is a procedure that can greatly overestimate their effect in a pulsed laser experiment. As a transform limited coupling laser is employed, the amount of dephasing over the laser pulse duration (the interaction time) is only of the order π radians and so is not significant.

The inverted matrix yields the steady-state values of the matrix elements. The relevant matrix element for the generation of the field at ω_g is ρ_{31}. The macroscopic polarization at ω_g is described in terms of the density matrix by the following expression:

$$P(\omega_g) = 2N\mu_{13}\rho_{13}. \tag{7}$$

Within the matrix element ρ_{13} are contained, to all orders, the terms relevant for calculating the dressed susceptibilities of the system, i.e., $\chi_D^{(1)}(\omega_g;\omega_g)$ and $\chi_D^{(3)}(\omega_g;2\omega_a,\omega_C)$. It is important to recognize that these quantities (even the ''linear'' terms $\chi_D^{(1)}$) are inherently nonperturbative since they include the interaction Ω_C to all orders.

In matching the calculations to the experiments, the modifications due to the Doppler effect must be incorporated into the susceptibilities. Random Doppler shifts due to the Maxwellian velocity distribution of the Kr atoms cause a distribution in the detunings [defined by Eq. (6)] for the ensemble of atoms. The response of the medium, characterized by the susceptibilities, at a given set of applied laser frequencies must therefore include the Doppler broadening via performing the weighted sum over these detunings. Due to the Gaussian form of the Maxwellian velocity distribution, the effect on susceptibilities from atoms in velocity classes significantly larger than the width of the distribution (i.e., giving rise to frequency shifts significantly larger than the Doppler width) will be negligible. The results, after Doppler averaging, for the susceptibilities Im $\chi_D^{(1)}$, Re $\chi_D^{(1)}$, and $\chi^{(3)}$ are shown in Fig. 2. The calculation was performed for $\Omega_C = 0.25$ cm^{-1} ($\Omega_C = 2.5\gamma_{\mathrm{Doppler}}$) and for $\Omega_C = 0.025$ cm^{-1} ($\Omega_C = 0.25\gamma_{\mathrm{Doppler}}$). This illustrates how for these conditions the values of $\chi_D^{(1)}$ are greatly reduced relative to the weak field case, while $\chi_D^{(3)}$ remains partially resonantly enhanced. For $\Omega_C = 0.25\gamma_{\mathrm{Doppler}}$ the absorption length in a medium of density 10^{16} cm^{-3} (typical value for density in these experiments) will be 2 μm. For $\Omega_C = 2.5\gamma_{\mathrm{Doppler}}$ this has increased by a factor of 6×10^3 to 12 mm. For a long medium [7] the

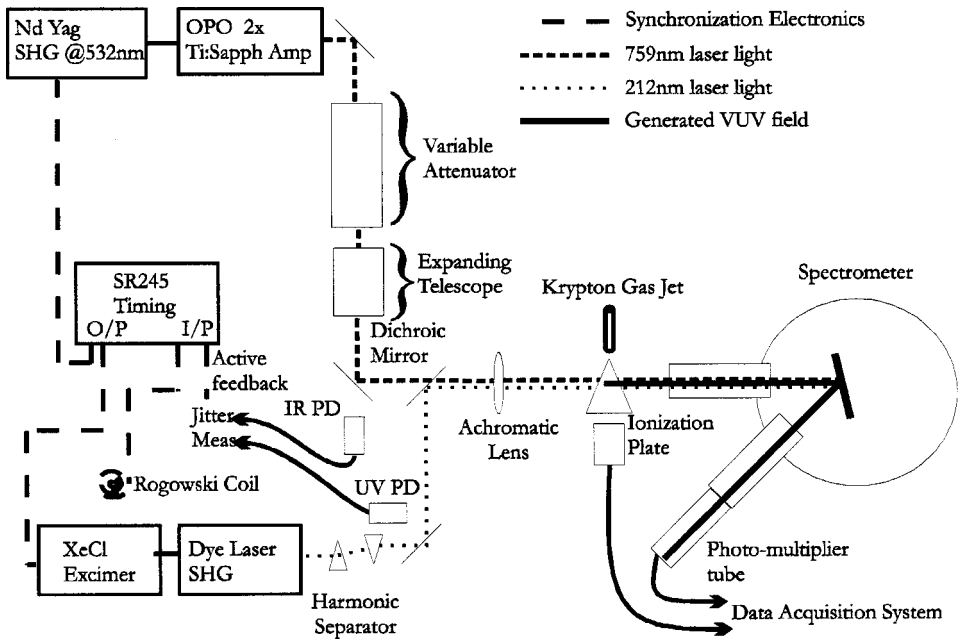

FIG. 3. A simplified schematic diagram of the experiment (not to scale). This illustrates how the main components of the experiment are integrated to provide temporal and spatial coincident laser pulses (at 212.55 and 759 nm) within the Kr medium (vacuum system omitted). The generated VUV light is separated from the input laser radiation using the spectrometer and detected by a solar-blind photomultiplier tube.

generated field intensity will scale with the value of $|\chi_D^{(3)}/\mathrm{Im}\,\chi_D^{(1)}|^2$. We see from the data in Fig. 2 that this parameter will increase by a factor of $\sim 10^3$ between $\Omega_C = 0.25\gamma_{\mathrm{Doppler}}$ and $\Omega_C = 2.5\gamma_{\mathrm{Doppler}}$.

The correct calculation of the intensity generated at ω_g proceeds by the substitution of these dressed and Doppler averaged susceptibilities into the propagation equation derived from Maxwell's equations:

$$\frac{\partial A_g}{\partial z} = i\,\frac{\omega_g}{4c}\,\chi_D^{(3)} A_a^2 A_C \exp[-i\Delta k_g z] - \frac{\omega_g}{2c}\,\mathrm{Im}\,\chi_D^{(1)} A_g + i\,\frac{\omega_g}{2c}\,\mathrm{Re}\,\chi_D^{(1)} A_g, \qquad (8)$$

where A_i's are the electric field amplitudes, and Δk_g the wave-vector mismatch for the generated field defined as $\Delta k_g = k_g + k_C - 2k_a$, where these wave vectors are also derived from the dressed and Doppler averaged susceptibilities. This equation can be solved analytically for a homogenous medium with a well-defined length and this operation was carried out (again using MATHEMATICA) to generate a general analytical expression for the intensity of the generated field. A fuller description of this procedure and the assumptions employed can be found in [19].

The calculations of generated field intensities are made under the assumption of monochromatic applied fields. This is consistent with the approach of Harris, Field, and Imamoglu [7] for the treatment of transform limited coupling. However, this ignores the issue of that portion of the two-photon field spectrum that may lie outside the transparency window and in the region where the phase matching is still poor.

III. DESCRIPTION OF THE EXPERIMENTAL APPARATUS AND PROCEDURES

Electromagnetically induced transparency depends upon the coupling laser field preparing atomic coherence, therefore the dephasing rates of these coherences are of critical importance in any experimental realization of EIT. A necessary condition is that the coupling field should be single mode and, if pulsed, be near transform limited. To achieve this we have employed a commercially available laser system comprising an optical parametric oscillator pumped by the second harmonic of an injection seeded Nd:YAG laser. The output of this laser was tunable in the range 750–850 nm and this capability was used in some of the experiments reported here. Most measurements were, however, made with the laser tuned close to (i.e., within the Doppler width of) exact resonance at 758.94 nm.

The experimental apparatus is shown in a simplified schematic form in Fig. 3. The optical parametric oscillator OPO was a Mirage 800 (Continuum) and was pumped by the second harmonic of a Powerlite 7010 (Continuum) injection seeded Nd:YAG laser that ran at a repetition rate of 10 Hz. The OPO cavity employed in this laser is kept short, with a mode spacing $\sim$3 GHz, and this facilitates the stable operation of the laser on a single mode [22]. Typically less than 25 mJ of green light was required to pump the oscillator. The output from the oscillator was amplified in a series of Ti:sapphire amplifiers, pumped by the remaining 532 nm radiation from the Nd:YAG. This system reliably operated on a single mode, with single mode operation that could be maintained even if the laser were tuned over a modest range of ± 20 cm^{-1} via the use of active feedback to the rear mirror. The pulse duration was <4 ns and it was believed to be close to the transform limit with a bandwidth of $\sim$200 MHz (0.007 cm^{-1}) [22]. The beam quality was about 1.5 times diffraction

limited and characteristically oval in shape.

This laser could generate pulse energies of up to 30 mJ at 758 nm, but typically for the experiments described in this paper the pulse energies employed were in the range 0.01–5 mJ. Nonetheless reduced shot-to-shot power fluctuations were found if the system were used with full amplification due to saturation and this was the usual mode of operation employed. The pulse energy could then be reduced to the desired range by using a variable attenuator comprising a half-wave-plate plus polarizer combination. Energies of pulses entering the interaction region were monitored on a shotwise basis by using a linear photodiode picking up light transmitted through one of the mirrors, and this photodiode was carefully calibrated against an energy meter so as to provide absolute values of laser pulse energy. Signals from the photodiode were sent to one of the channels of a gated integrator for digitization and recording by the data acquisition system.

The detuning of the coupling laser from the $|2\rangle$-$|3\rangle$ transition frequency is a critical parameter in these measurements. It was therefore necessary to establish this detuning for a given measurement to a precision of better than 0.05 cm^{-1} (i.e., half the Doppler width of the transition). To achieve this a laser-induced fluorescence technique was adopted. A Kr-Ne–filled hollow-cathode discharge lamp was used to excite Kr atoms to the $|2\rangle$ and $|3\rangle$ states of the scheme. A small fraction of the coupling laser beam could be diverted to be focused into this lamp. As the coupling laser was scanned across the $|2\rangle$-$|3\rangle$ transition an enhanced laser-induced fluorescence signal was detected at 90° to the laser beam direction using a photomultiplier tube. The width of this proved to be comparable to the Doppler width of the transition and so the LIF signal could be used as a frequency reference of the required precision.

In contrast to the OPO laser described above, the UV field (ω_a) need not be transform limited for EIT to occur. However, that part of the UV laser bandwidth that lies outside the transparency window and in regions where phase matching is still poor will not effectively contribute to four-wave mixing [7]. The laser field at 212.55 nm (i.e., the two-photon resonance) was provided by frequency doubling the output of an excimer pumped dye laser. The dye laser was operated with an intracavity étalon that ensured a fundamental (425 nm) bandwidth of ~1.5 GHz, but the laser output was nevertheless multimode. Second harmonic pulse durations of approximately 12 ns were measured. The dye used was Stillbene 3 dissolved in methanol, and was found to generate second harmonic pulses of up to 250 μJ from the 425-nm fundamental. Subsequently better performance was found by using Exalite 428 in 1,4-dioxane with UV pulse energies in excess of 500 μJ being possible and longer dye lifetime performance. Far lower pulse energies (typically <100 μJ) were delivered to the interaction region owing to losses in the prisms used for the separation and beam transportation optics.

Precise synchronization between the two laser pulses in the interaction region was essential for four-wave mixing. This was achieved with a shot-to-shot variation of interpulse timings of less than 4 ns. Optimal results were obtained by triggering the Nd:YAG laser *Q* switch with a Stanford Research System (SRS) delay generator, which was triggered by picking up rf noise generated by the triggering of the thyratron in the excimer laser. The delay between the thyratron noise trigger and the Nd:YAG trigger was actively modified on a shot-to-shot basis by the data acquisition system, which analyzed the delay between the pulses using an Ortec 567 time-to-analogue converter. The pulses were detected by two photodiodes, and the delay between them generated a pulse proportional to the time difference, which was actively minimized by the acquisition software. This minimization routine effectively eliminated systematic drifts, but a residual stochastic jitter of ± 2 ns remained. The pulsed gas jet was also triggered by the SRS delay generator.

The laser beams were combined with parallel vertical polarizations at a dichroic mirror (high 45° reflectance 212 nm, high transmission for 758 nm). This permitted collinear alignment with well-overlapped beams in the interaction region. Both beams were focused using an $F = 30$ cm lens. Due to the adjustment of the coupling laser beam divergence using a preceding telescope the focus of this beam was displaced from that of the UV laser, the latter being focused to the center of the interaction region. The UV laser beam in the interaction region was thus completely enclosed within the area of the coupling laser beam which had a diameter of several millimeters at this location. Both beam profiles were measured at a plane equivalent to the position of the interaction region using a charge-coupled-device (CCD) camera coupled to a PC with image processing software. The UV beam was sufficiently intense that the fluorescence from the thin glass plate in front of the CCD generated enough light to generate an image. The spot focal diameter of the UV beam was measured to be 120 μm and was consistent with the beam focus being $2\times$ diffraction limited. For the coupling beam wavelength the CCD array was sensitive and an accurate beam profile was obtained; this profile was approximately Gaussian in form and the diameter was 3 mm. From this information we were able to establish the value of the coupling beam intensity in the interaction region to within a factor of 2 leading to values of Ω_C established to an accuracy of better than $\pm 50\%$.

A pulsed gas valve fitted with a 30 mm syringe needle (in order to deliver the gas close to the UV laser beam waist) was used to supply the Kr gas. The valve was backed by pressures in the range of 1–2 bar and the gas density provided immediately below the needle was estimated [23] to be in the range 10^{16}–10^{17} cm^{-3} and to extend over path lengths of from ~0.1–0.5 cm. The gas density from this valve was not uniform: it has a spreading angle of up to 45°, which we believe leads to an approximately Lorentzian density distribution. Despite this, the gas valve has a number of advantages compared to a cell, for instance permitting reliable determination of the laser intensities throughout the short interaction zone and allowing, in principle, the study of XUV as well as VUV production. The density of gas from the needle will fall off approximately as the inverse square of the distance from the orifice if the spreading angle remains constant and the expansion self-similar. The density-path length product will thus decrease approximately as the inverse of this distance from the orifice. Knowledge of this simple scaling was used to vary the conditions of the experiment in order to make comparisons between high- and low-density conditions.

Photoions are generated by the UV laser field and were collected by electrodes located close to the interaction region. We were able to study the photoionization simultaneously with the VUV radiation generated by four-wave mixing. More importantly this facility was used to determine the laser frequency for exact two-photon resonance for the UV laser (ω_a). The two-photon resonance condition was established by measuring the two-photon enhanced, three-photon ionization signal in the absence of any coupling field. The most precise determinations of the two-photon resonant frequency were made with relatively low gas jet backing pressure and small UV pulse energies to minimize the effects of pressure or power broadening of the resonant photoionization profile. We estimate that by this procedure the laser frequency could be set to within 0.05 cm^{-1} of exact resonance (i.e., within the laser bandwidth and Doppler width).

The interaction region lay 10 cm from the entrance focal plane of a 1-m focal length VUV monochromator (Seya mounting), which was used to collect efficiently the generated VUV and to separate the generated field from the laser fields. The monochromator was fitted with a 1200 line/mm diffraction grating, but because of previous laser-induced damage to the optical surface of this grating, the reflectivity of the diffracted first order was not uniform across this surface. Detection of the VUV pulses was performed with a solar blind VUV sensitive photomultiplier tube (PMT) (Thorn EMI G26E314) operated in the linear region. Two interference filters were placed in front of this PMT to increase the rejection of the scattered 212 nm radiation (for which the detector still has significant residual sensitivity). This detection system was linear but no absolute calibration of its spectral response was available, so no absolute VUV power measurements were possible. Strong reabsorption of the resonant VUV was found to be caused by residual levels of Kr gas (background pressure 10^{-4} mbar) outside of the interaction region (i.e., along the 2-m path length in the monochromator). To eliminate this, a MgF_2 window forming a vacuum seal to isolate the interaction region from the monochromator was placed in the beam path a few centimeters after the gas jet, and this prevented any background Kr density in the monochromator. An auxiliary determination of the single-photon resonance condition ($|2\rangle$-$|3\rangle$) was achieved by performing a VUV experiment with the MgF_2 window removed so that strong reabsorption of the generated field was observed, in regions where the strong coupling laser was absent. This absorption dip was observed when the OPO system was tuned while holding the other laser at two-photon resonance ($|1\rangle$-$|2\rangle$).

The data acquisition system was comprised of several gated integrators (SRS 250). Initially these were set up using the signals recorded by a fast digital oscilloscope (Tektronix 620) to locate the gate pulses in the correct locations and to optimize their duration. This system permitted simultaneous acquisition of photoionization signals, generated VUV signals, time delays between pulses and the coupling laser energy. The simultaneous record of laser pulse energies and the VUV signal enabled the study of correlation between these parameters. It was also necessary to monitor the variation in time delay (± 2 ns) between the two laser pulses that arose from the jitter between the Nd:YAG and Excimer lasers, as well as the laser pulse energies.

The coupling beam strength was adjusted (using the wave-plate/polarizer combination) over a range of Rabi frequencies from $\Omega_C = 0$ to 2 cm^{-1}. For the measurements of the VUV intensity dependence on the coupling field strength the following procedure was adopted to acquire the data. By random adjustments of the rotation stage in which it was mounted the wave-plates orientation could be varied so as to generate a random series of pulse energies across the range of interest. Acquiring many data points (>1000) per run in practice meant that all the possible values of laser energy were thus sufficiently sampled during a given experiment, however these were weighted more to low values of laser power. For each laser shot the value of the pulse energy and the VUV intensity were individually digitized and recorded as an array for subsequent analysis. The analysis was performed by taking the adjacent point average for the VUV signal over 20 points clustered around a particular pulse energy value and it is this data that is plotted in Sec. IV. By this technique an energy resolution of 2% of the full range of energy was obtained. For the lower energies in the range the effective resolution was several times better than this, e.g., for a 0–0.5 mJ full range this was a resolution of <10 μJ at low energies. It should be noted that the shot-to-shot fluctuation in the VUV signal is always substantial in these measurements due to the sensitivity of the nonlinear mixing, e.g., to the UV laser energy and beam profile. Therefore there is a level of noise retained in the data that could only be reduced by further averaging, which would consequently worsen the energy resolution.

To investigate the dependence of the VUV intensity on the UV laser power the following method was adopted. In contrast to the case with the coupling laser wave plates and polarizers for 212 nm were not available to us, so an alternative technique had to be found to allow smooth variation of the laser power. To do this the doubling crystal was moved slightly off of the optimum angle and so that the UV pulse energy was decreased. By variation of the crystal angle a range of UV laser pulse energies could be produced and these were measured using an energy meter. Unfortunately only at the optimum angle was the UV beam quality good. The beam quality deteriorates significantly as the angle is increased from the optimum. This led to uncertainty about the relative intensity within the interaction region of the experiment.

Relative VUV yield measurements were carried out to compare the conversion efficiency of the four-wave mixing process with both lasers on resonance ($\lambda_a = 212.55$ nm and $\lambda_C = 758.94$ nm) and for the case for which the coupling laser was detuned far from resonance ($\lambda_C = 840$ nm) but the other laser held at two-photon resonance ($\lambda_a = 212.55$ nm). The generated VUV was produced at wavelengths of $\lambda_g = 123.6$ nm and $\lambda_g = 121.7$ nm, respectively, in these two cases, the latter value was chosen since previous work investigating the conversion efficiency of this mixing scheme has already been carried for this scheme under comparable conditions. To make a comparison, all experimental conditions were kept constant aside from the detuning of the coupling laser, the coupling laser pulse energy and the monochromator exit slit width. The latter two parameters had to be increased significantly from the values used for the resonant lasers in order to record a measurable signal in the nonreso-

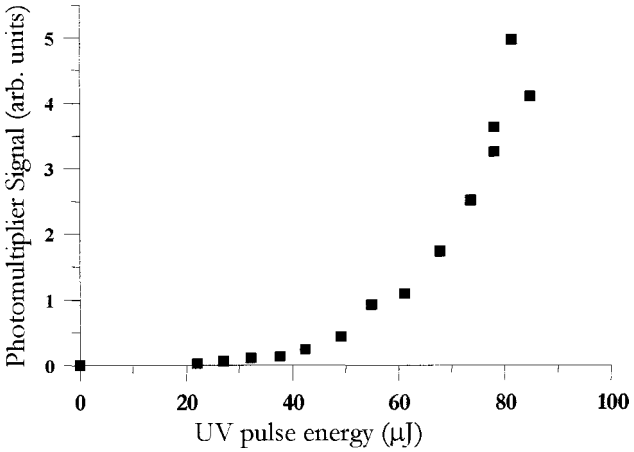

FIG. 4. Intensity of generated VUV vs the UV (212.55 nm) pulse energy (μJ) at the interaction region. The coupling laser energy was 2.5 mJ. Note that even with the highest UV laser power used ($\sim$5 kW) there is no evidence for saturation in the VUV signal.

nant case. It was assumed that the spectral dependence of the diffraction grating reflectivity, interference filters transmission (bandwidth specified to be $\pm$3 nm), and photomultiplier sensitivity are fairly independent of wavelength between 121.6 and 123.6 nm, an assumption we believe to hold to within a factor of 2.

IV. RESULTS AND DISCUSSION

A. Dependence of four-wave mixing on UV pulse energy

The dependence of the VUV pulse energy, determined by the signal output from the photomultiplier, on the UV laser pulse energy was measured. This was primarily to determine whether there was any evidence for saturation at high UV powers, e.g., due to photoionization. The results of this are shown in Fig. 4. As explained above the maximum UV power delivered to the interaction region was limited by losses in the steering optics and by the low conversion efficiency of the frequency doubling. The range of UV pulse energies shown in Fig. 4 is therefore between 0 and 75 μJ, as the UV laser power was varied the coupling pulse energy was kept constant at 2.5 mJ. The significant feature that can be noted from the curve in Fig. 4 is that there is no indication that the four-wave mixing is saturating, even for the highest UV energies employed.

The absence of saturation in the VUV signal versus UV pulse energies demonstrates that a number of potentially detrimental effects are not significant under the experimental conditions investigated. Since the UV field can cause direct single-photon ionization for any atoms excited into state $|2\rangle$, there is, in principle, an extra dephasing channel for the $|1\rangle$-$|2\rangle$ coherence (ultimately responsible for the destructive interference that causes EIT) from this photoionization rate. This dephasing (depopulation) rate Γ_{ion} will be significant if it approaches the value of the leading spontaneous decay rate, i.e., Γ_3; if these become comparable, the destructive interference leading to EIT will no longer be significant. The lack of saturation in the curve of Fig. 4 indicates that this situation is not reached in our experiments. This is further corroborated by an estimate of the ionization rate in the experiment. For the measured focal spot diameter of 120 μm the maximum UV laser intensity for any of the experiments can be estimated to be 4×10^7 W cm^{-2}. Taking calculated ionization rates for the $5p$ $[0,\frac{1}{2}]$ state of Kr (Hoffsaes, [25]) we obtain an upper limit for the ionization rate in our experiments of $\Gamma_{\text{ion}}=8.7\times10^7$ s^{-1}, which is still only $\frac{1}{3}$ the value of Γ_3.

The UV field (at frequency ω_a in Fig. 1) in this four-wave mixing process will interact with the dressed atom in a fashion adequately described by lowest-order perturbation theory. To be explicit the process involves the interaction of two photons from the UV field, i.e., is second order in perturbation theory. This was confirmed by calculations that were made using our model. For these higher-order terms in the UV laser coupling strength were retained. Over the range of laser powers pertinent to these experiments a quadratic form was found from these calculations for the VUV power dependence on the UV power. In contrast, for UV powers several orders of magnitude higher than those used in these experiments the calculations reveal considerable deviations from quadratic behavior [19]. Earlier work on four-wave mixing in Kr employing the same two-photon resonance, but with the second laser tuned far from single photon resonance, found essentially a quadratic dependence [24]. We observe in fact a steeper than quadratic dependence (closer to the fourth power) of the generated VUV signal on the UV pulse energy. This probably arises as an experimental artefact due to the method of UV pulse energy variation that we have employed. This can lead to the UV intensity being affected disproportionately relative to the pulse energy as the beam quality deteriorates. This does not, however, effect our conclusion drawn above regarding the absence of saturation.

B. Dependence of four-wave mixing on coupling laser energy

We will now consider the data for the dependence of the intensity of the generated VUV radiation on the pulse energy of the coupling laser. Figure 5 shows the measured VUV signal as a function of coupling laser energy for two values of coupling laser detuning (i) on resonance (detuning 0.0 cm^{-1}) and (ii) off resonance by $+0.035$ cm^{-1} ($\approx\frac{1}{2}\gamma_{\text{Doppler}}$), in both cases the other laser remained at exact two-photon resonance. Also shown on the horizontal axis is the coupling field Rabi frequency Ω_C computed from the pulse energy and measured spot size/pulse duration data. These results show that a small VUV signal is generated up to values of laser energy of 20 μJ ($\Omega_C=0.025$ cm^{-1}) above which the VUV signal rises sharply until an IR pulse energy of around 200 μJ ($\Omega_C=0.1$ cm^{-1}). Above this laser pulse energy the rise in VUV signal becomes less steep and eventually levels off. For the exactly resonant coupling ($\Delta=0.00$ cm^{-1}) the onset of the sharp rise is at noticeably lower coupling laser powers, and is steeper, than for the off-resonant ($\Delta=0.035$ cm^{-1}) case. The maximum VUV signal level attained on resonance is also significantly higher (a factor of around 1.2 times larger) than for the off-resonant case.

In contrast to the dependence of the four-wave mixing on UV power (see Sec. IV B) the IR power dependence data cannot be simply explained within the framework of lowest-order perturbation theory. If the coupling laser were interact-

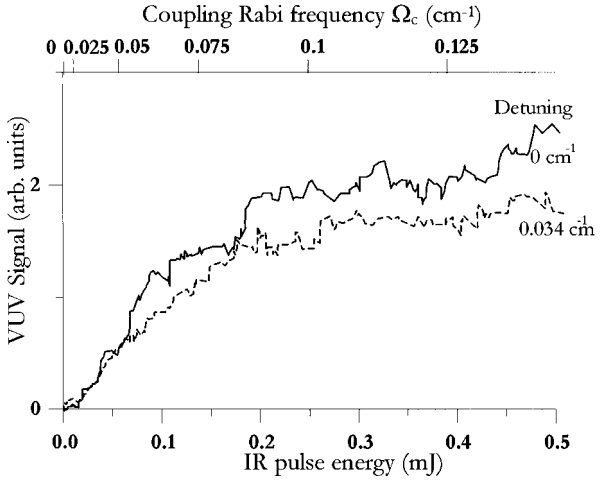

FIG. 5. Generated VUV intensity vs the pulse energy of the coupling laser (mJ). The equivalent Rabi frequency (cm^{-1}) is given along the upper scale. Results for two coupling laser detunings (i) $\Delta_C = 0.00\ cm^{-1}$ (solid curve) and (ii) $\Delta_C = 0.034\ cm^{-1}$ (dotted curve) are shown. These show broadly similar behavior, but the exactly resonant data show lower VUV signals at the smallest coupling strengths compared to the detuned case. In contrast the VUV signal for zero detuning reaches higher values at larger coupling laser strengths.

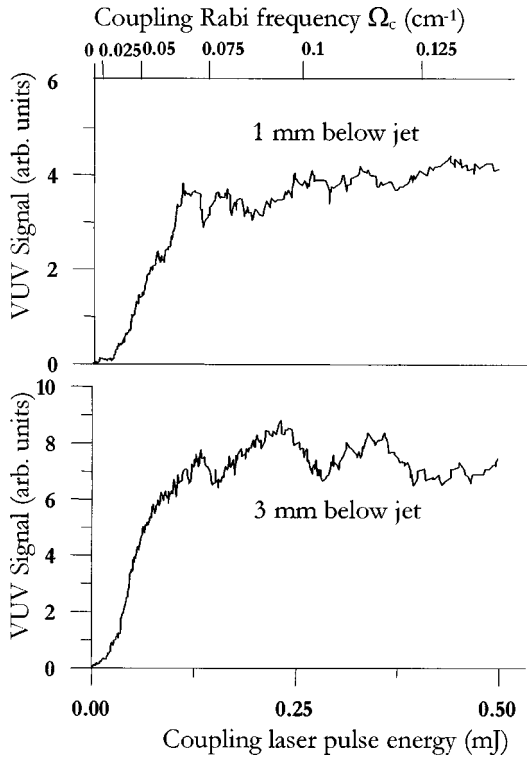

FIG. 6. Density dependence of the generated VUV signal vs the coupling laser power. Graph (i) (upper frame) shows data obtained with the interaction region located 1 mm below the gas jet orifice. Graph (ii) (lower frame) was obtained with the interaction region 3 mm below the orifice. Using the scalings discussed in the text we can deduce that the conditions for curve (i) were approximately 10 times more dense than for graph (ii), with an *NL* product value three times larger than for graph (ii).

ing with the atom in this four-wave-mixing scheme in a perturbative limit, then the scaling of VUV signal with laser power should be linear up to some intensity at which saturation effects would start to become evident. The observed behavior is in direct contrast to this, with an initially low value of generated VUV signal followed by a sharp rise then a gradual roll off.

A more detailed examination of the behavior at low coupling strengths (with a consequently higher-energy resolution of $\sim 5\ \mu J$) is shown in Fig. 6. Here it can be seen that at very low Rabi couplings and with the coupling laser on resonance ($\Delta_C = 0.0\ cm^{-1}$) there is some VUV signal generated even at very low coupling laser energies. But then a clear gradient change is apparent in these data around 25 μJ with a steep rise in the VUV signal.

Two sets of data are shown in Fig. 6, one (i) for frequency mixing when the interaction region was 1 mm below the gas jet orifice and the other (ii) for when the interaction region 3 mm below. Note a direct comparison of the intensities in these two sets of data is not possible due to the nonuniformity of the reflection efficiency of the diffraction grating. The value of the integrated density-length product along the propagation axis will fall off simply as the inverse of the distance below the orifice. Therefore the density-length product for (i) will be three times that for (ii), implying the initial opacity of the sample at 123.6 nm (i.e., before the coupling laser was applied) will be similarly larger for (i). These differences in density-length product are reflected in differences in the data for the VUV versus IR pulse energy. The laser energy at which (i) starts to rise sharply ($E_C = 20\ \mu J$) is higher than that at which curve (ii) shows a sharp rise ($E_C = 10\ \mu J$). An estimate of the density in the region 1 mm below the gas jet orifice ($2 \times 10^{16}\ cm^{-3}$) indicates that the preparation energy required [14] for transparency is $\sim 30\ \mu J$. This is in reasonable agreement (given the uncertainties in the gas density) with the experimental result. Moreover, given that the *NL* product is inversely dependent on distance below the orifice, the absence of a discernible sudden turn on at 3 mm below the jet is consistent with the smaller preparation energy constraint. Thus for this latter data set we should expect a closer agreement with the theoretical calculation which does not include a preparation energy condition.

For the data taken with the interaction region 3 mm below the gas jet orifice the increased conversion efficiency corresponding to the sharp rise in the generated VUV signal occurs at the coupling strength predicted by the theory of nonlinear mixing with EIT discussed in Sec. II. Specifically we expect a large enhancement in the conversion efficiency between $\Omega_C = 0.25\gamma_{\text{Doppler}}$ and $0.5\gamma_{\text{Doppler}}$. In these experiments $\gamma_{\text{Doppler}} = 0.1\ cm^{-1}$. Examination of the data in Fig. 6 (ii) enables us to make an estimate of the increase of the conversion efficiency as Ω_C is increased. The VUV signal between the Rabi coupling strengths of $0.25\gamma_{\text{Doppler}}$ and $0.5\gamma_{\text{Doppler}}$ increases by a factor >20. Over the same range the laser energy increases by a factor of only 4. This implies a >5 times increase in the conversion efficiency over this range of coupling laser energies.

A calculation including phase-matching and Doppler broadening was made of the VUV signal as a function of the coupling field strength. For this calculation a uniform gas distribution is assumed with a density of $2 \times 10^{15}\ cm^{-3}$ and a path length of 3 mm. These conditions are considered typical

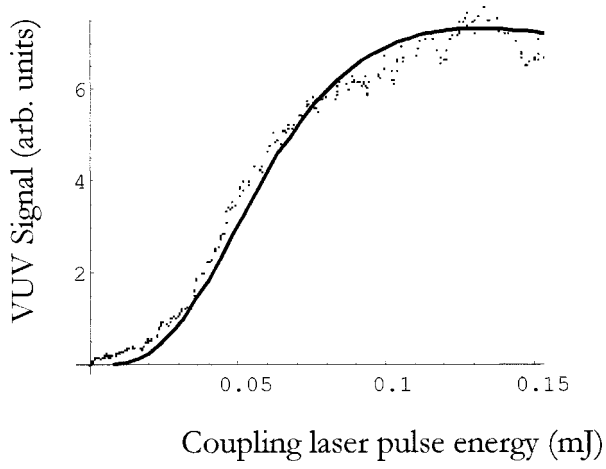

FIG. 7. Results of theoretical modeling the generation of VUV compared to typical experimental data. For the calculation the gas was assumed to be of uniform density (2×10^{15} cm^{-3}) over a path length of 3 mm. The calculated curve (solid line) matches the experimental data (dotted line) over most of the coupling laser energy range shown (a vertical scaling was applied to the calculated data). For the lowest coupling laser powers (pulse energies below 25 μJ) the measured signal generated is larger than the theoretical prediction. We attribute this difference to the effects of the nonuniform gas density employed in the experiment.

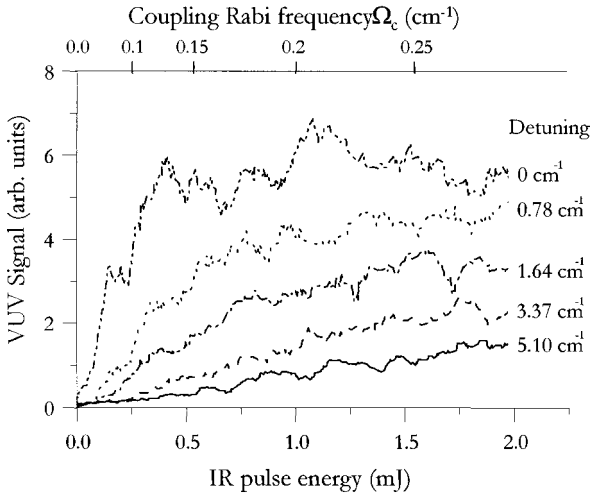

FIG. 8. Dependence of the generated VUV signal against coupling laser power for a range of values of coupling laser detuning (Δ_C) between 0 and 5.1 cm^{-1}. The data for large detunings shows a close to linear dependence of the VUV signal on coupling laser energy.

for a distance several millimeters below the gas jet needle. A monochromatic UV field is assumed; we have found that this is adequate to model the initial rise in the VUV conversion efficiency. We calculate that off-resonant components of the UV field contribute little to the generated field until higher coupling field strengths are reached, when transparency is obtained and phase mismatch overcome. The laser pulse duration and diameter were taken to have the same values as measured for the experiment, thus we can make a direct comparison with the laser pulse energies used in the experiment. The result of this calculation is shown in Fig. 7, with data from curve (ii) of Fig. 6 given for comparison. The vertical axis (VUV signal) for the calculated data has been scaled to match the peak values of the experiment. The calculation does not attempt to predict an absolute VUV power due to the large uncertainty in the gas density.

The calculation can be seen to reproduce well the main features of the experimental data. In particular, the points at which the VUV signal starts to rise steeply and then to roll off are in close agreement. At very low laser coupling strengths (<25 μJ), however, the theoretical values are very low (effectively zero on this linear scale) while the experimental data shows some VUV light is generated. We believe this arises because the gas density distribution is not uniform as assumed in the calculation. The calculation predicts essentially negligible VUV generation for laser coupling strengths below the Doppler width. In contrast for the experiment there is always some finite signal generated due to the lower-density regions of gas at the edges of the density distribution. The calculation also ignores the temporal dependence of the laser interactions, the laser linewidths (i.e., the possibility of extra phase diffusion during the laser pulse duration) and the effects of ionization. Further development of our calculations to include some of these effects and experiments in a sample with a uniform gas density is the subject of ongoing work.

The change in the conversion efficiency as a function of the coupling laser power gives a figure of merit as to the effectiveness of the EIT in enhancing the nonlinear mixing. Larger factors than those observed should be possible; in particular, an increase should be achieved if the optimum density-length product (NL) is employed in the experiments. Our estimates of the density-length product involved in the experiments at the present time would indicate that this quantity is presently $<10^{16}$ cm^{-2}. Estimates can also be made of the optimal NL product [26] that should be used, use of greater values of NL will be limited either by the absorption of the generated field or residual phase mismatch of the field at 212 nm. The latter constraint places the NL limit as that which would cause an additional factor of π phase shift in the 212 nm field, a value that turns out to be 2×10^{17} cm^{-2} in these experiments. A more stringent constraint is set by the absorption due to imperfect EIT caused by the photoionization rate $\Gamma_{\rm ion}$ [27]. Assuming that the value of $\Gamma_{\rm ion}/\Gamma_2=0.1$ (close to the situation in the experiment) with a Rabi coupling of $\Omega_C=1.7$ cm^{-1} this leads to an estimated optimal value for the density length of 6×10^{16} cm^{-2}. Since this value of Rabi coupling (and greater) are easily achieved with our laser it would seem that there is scope to achieve larger increases in the efficiency by increasing N or L.

An investigation was also carried out into how the VUV signal enhancement depended upon the detuning for large detunings from resonance. The expectation here is that for increasing detunings the resonant four-wave mixing from a dressed atom behavior will evolve smoothly into off-resonant four-wave mixing from a bare atom. This is seen in Fig. 8. For the on resonant case, the behavior described above is again apparent, while for a large detuning (3.37 and 5.1 cm^{-1}) a linear dependence of VUV signal on coupling strength was found. At moderate detunings (0.78 and 1.64 cm^{-1}) an intermediate behavior was followed.

C. Relative conversion efficiency measurement: on-resonant vs off-resonant frequency mixing

The conversion efficiency of the resonant frequency-mixing scheme, enhanced as it is by EIT, ought to be much higher than a nonresonant scheme. We have made a quantitative comparison of the VUV yield obtained both on and 1270 cm^{-1} off resonance. Specifically we have compared the VUV yield of the fully resonant scheme with the coupling laser at 759 nm to that when the two-photon resonance was maintained but the ''coupling'' laser was detuned far from single-photon resonance to 840 nm. Earlier work [6] has shown that by optimization of the Kr pressure in a cell the two-photon resonance enhanced sum-difference mixing in this krypton scheme can yield conversion efficiencies for the generation of radiation at 121.7 nm (''coupling'' laser at 840 nm) in the range 10^{-4} [6]. Under the present conditions of mixing in a lower-density gas jet a lower conversion efficiency is expected for this ''off-resonant'' nonlinear scheme with conversion efficiencies 10^{-5}–10^{-6}.

In these experiments the coupling laser is unfocused and so the yield of VUV is low in the case of off-resonant coupling field (at 840 nm). To permit a comparison it was therefore necessary to increase the coupling laser energy to 7 mJ from the optimum value of the resonant case, which was 0.2 mJ. At the same time the monochromator exit slit widths had to be opened from 0.25 mm (759 nm) to 2 mm (840 nm) to obtain a measurable signal. Under these conditions the VUV signal measured at resonance (759 nm) was found to be a factor of 350 ± 100 larger than that measured with the laser detuned to 840 nm. This was despite using a far lower laser energy to generate the VUV radiation at resonance (0.2 mJ as opposed to 7 mJ). As the VUV yield scales essentially linearly for a detuned coupling laser (see above) we can therefore make an estimate of the relative conversion efficiencies between on and off resonant cases, the ratio of these being $(1.2 \pm 0.3) \times 10^4$.

V. CONCLUSIONS

We have investigated the VUV radiation generated via resonant four-wave sum-difference frequency mixing in Kr. The Kr gas in these experiments was in a pulsed gas jet expanding into a vacuum chamber. A detailed study was made of the dependence of the generated field intensity on the intensities of the laser fields driving the mixing scheme. The variation of the generated intensity with coupling laser field strength shows a clear signature for EIT (see Figs. 5 and 6) in good agreement with theoretical predictions (Fig. 2). In particular, the signal shows an increase in conversion efficiency where the coupling Rabi frequency Ω_C approaches the Doppler width of the 123.6-nm transition (0.1 cm^{-1}).

Fivefold EIT enhancements are estimated from the experimental data. This measured enhancement is significantly less than predicted from our elementary theoretical treatment. There may be additional factors at play in the experiment that are not included in our simplified theory. In particular, the gas density distribution, excess laser linewidth, and photoionization rate due to the UV laser may be important in the experiment but are ignored in the theory. Further work is underway to investigate the importance of these factors.

The enhancement in the conversion efficiency for resonant frequency mixing is quantified in comparison to the nonresonant case. Enhancement factors of 10^4 are established. A significant contribution to this resonant enhancement can therefore be attributed to the EIT effect.

ACKNOWLEDGMENTS

We would like to take this opportunity to acknowledge the very useful discussions with Professor Stephen Harris at several points during this work, and to acknowledge Professor Peter Knight for his invaluable advice on the manuscript. We also thank Christoph Keitel and Jason Petch for early work on the calculations and Ibrahim Kucukkara, Martin Archbold, and Sebastian Echaniz for valuable help with the experiments. We are indebted to Peter Ruthven and Shahid Hanif for their technical assistance. We would especially like to thank Professor Hofsaess for providing us with data for the ionization of krypton. The U.K. Engineering and Physical Sciences Research Council supported this work.

[1] Y. R. Shen, *The Principles of Non-Linear Optics* (Wiley, New York, 1985).
[2] C. R. Vidal, in *Tunable Lasers*, edited by L. F. Mollenauer and J. C. White, Springer-Verlag Topics in Applied Physics Vol. 59 (Springer-Verlag, Berlin, 1987), Chap. 3; J. F. Reintjes, *Nonlinear Optical Parametric Processes in Liquids and Gases* (Academic, New York, 1984).
[3] J. F. Young, G. C. Bjorklund, A. H. Kung, R. B. Miles, and S. E. Harris, Phys. Rev. Lett. **27**, 1551 (1971).
[4] D. J. Brink and D. Proch, Opt. Lett. **7**, 494 (1982).
[5] R. Hilbig and R. Wallenstein, IEEE J. Quantum Electron. **QE-19**, 194 (1983).
[6] J. P. Marangos, N. Shen, H. Ma, M. H. R. Hutchinson, and J. P. Connerade, J. Opt. Soc. Am. B **7**, 1254 (1990).
[7] S. E. Harris, J. E. Field, and A. Imamoglu, Phys. Rev. Lett. **64**, 1107 (1990).
[8] A. Imamoglu and S. E. Harris, Opt. Lett. **14**, 1344 (1989).
[9] B. Lounis and C. Cohen-Tannoudji, J. Phys. II **2**, 579 (1992).
[10] J. J. Macklin and S. E. Harris, Phys. Rev. A **40**, 4135 (1989).
[11] K.-J. Boller, A. Imamoglu, and S. E. Harris, Phys. Rev. Lett. **66**, 2593 (1991).
[12] J. E. Field, K. H. Hahn, and S. E. Harris, Phys. Rev. Lett. **67**, 3062 (1991).
[13] M. Jain, G. Y. Yin, J. E. Field, and S. E. Harris, Opt. Lett. **18**, 998 (1993).
[14] S. E. Harris and Z.-F. Luo, Phys. Rev. A **52**, R928 (1995).
[15] G. Z. Zhang, K. Hakuta, and B. P. Stoicheff, Phys. Rev. Lett. **71**, 3099 (1993).
[16] G. Z. Zhang, M. Katsuragawa, K. Hakuta, R. I. Thompson, and B. P. Stoicheff, Phys. Rev. A **52**, 1584 (1995).
[17] R. S. D. Sihombing, M. Katsuragawa, G. Z. Zhang, and K.

Hakuta, Phys. Rev. A **54**, 1551 (1996).
[18] G. Z. Zhang, D. W. Tokaryk, B. P. Stoicheff, and K. Hakuta, Phys. Rev. A **56**, 813 (1997).
[19] J. C. Petch, C. H. Keitel, P. L. Knight, and J. P. Marangos, Phys. Rev. A **53**, 543 (1996).
[20] W. R. Hindmarsh and J. M. Farr, in *Progress in Quantum Electronics*, edited by J. H. Sanders and S. Stenholm (Pergamon, New York, 1972), Vol. 2, p. 141.
[21] H. Haken, *Handbuch der Physik*, edited by S. Flugge (Springer, Berlin, 1970), Vol. 25/2c.
[22] W. R. Bosenberg and D. R. Guyer, J. Opt. Soc. Am. B **10**, 1716 (1993).
[23] A. H. Kung, Opt. Lett. **8**, 24 (1983).
[24] X. Xiong, Ph.D. thesis, University of Maryland (1991).
[25] D. Hofsaess (private communication); see D. Hofsaess, At. Data Nucl. Data Tables **24**, 285 (1979).
[26] S. E. Harris, G. Y. Yin, M. Jain, Hui Xia, and A. J. Merriam, Philos. Trans. R. Soc. London, Ser. A **355**, 2291 (1997).
[27] S. E. Harris (private communication).